

1

2

[JGR Biogeosciences]

3

Supporting Information for

4

[Hillslopes in Headwaters of Qinghai-Tibetan Plateau as Hotspots for Subsurface Dissolved Organic Carbon Processing during Permafrost Thaw]

5

6

[Yuqin Sun^{1,2,3}, Kale Clauson⁴, Min Zhou¹, Ziyong Sun⁵, Chunmiao Zheng^{2,3} and Yan Zheng^{2,3*}]

7

[¹ College of Engineering, Peking University, Beijing, 100871, China.

8

² State Environmental Protection Key Laboratory of Integrated Surface Water-Groundwater Pollution Control, School of Environmental Science and Engineering, Southern University of Science and Technology, Shenzhen, 518055, China.

9

10

³ Guangdong Provincial Key Laboratory of Soil and Groundwater Pollution Control, School of Environmental Science and Engineering, Southern University of Science and Technology, Shenzhen, 518055, China.

11

12

⁴ School of Earth and Environmental Sciences, Queens College, City University of New York, Flushing, NY 11367, USA.

13

⁵ School of Environmental Studies, China University of Geosciences, Wuhan 430074, China.]

14

Contents of this file

15

16

Text S1 to S3

17

Figures S1 to S6

18

Tables S1 to S3

19

20

Additional Supporting Information (Files uploaded separately)

21

22

Captions for Datasets S1 to S2

23

Introduction

24

Supporting information contains descriptions of sampling protocols, field and laboratory measurement details (Text S1), soil incubation experimental procedure (Text S2) and results (Text S3). Figures S1 and S6 illustrates the variations of SUVA₂₅₄ FI and BIX. Figure S2 depicts the soil incubation experiment set up. Figures S3 – S5 show fluorescent characteristics of the DOM samples and PARAFAC modeling results. Tables S1 reports uncertainties of endmember compositions and analysis. Table S3 and Figure S7 report soil incubation experimental data. Dataset S1 to S2 (separate electronic files) are original data of field and laboratory measurements of water chemistry parameters for all samples.

25

26

27

28

29

30

31

32 **Text S1. Sampling and Measurements.**

33 Temperature (T), electrical conductivity (EC) and pH were measured in the field using WTW-
34 COND-3301 instrument in 2012 and 2013, and Thermo 520M-01A instrument in 2018. Alkalinity
35 was measured using titration method in the field [Gran, 1952]. All samples were stored on ice at
36 4°C for shipment to laboratory.

37
38 Stable isotopes (δD and $\delta^{18}\text{O}$) were measured for samples collected in July 2013, and
39 September of 2013 and 2018 on a water isotope spectrometer analyzer (Model PICARRO L2130-
40 l) at Pri-ecoco, Beijing, China. Three standard solutions (GBW58, GBW59, and GBW60) were
41 employed as daily QA/QC. Each sample was analyzed 6 times and the result was calculated as the
42 average of the last three injections. The relative standard deviation (RSD) for duplicate analysis
43 was < 0.8%. The isotope compositions are expressed as the δ -notation related to Vienna Standard
44 Mean Ocean Water (VSMOW) in ‰.

45
46 DOC concentrations for samples collected in 2012 and 2013 were measured on a TOC-5000
47 Analyzer (Shimadzu) at both the Environmental Engineering Laboratory, Peking University and
48 Queens College, CUNY according to a Non Purgeable Organic Carbon (NPOC) method. Samples
49 collected in 2018 were analyzed by a TOC-L Analyzer (Shimadzu) at Southern University of Science
50 and Technology following the same protocol. Samples were analyzed in triplicate with the RSD
51 less than 3% as a threshold for accepting the result.

52
53 Measurement of cations was performed using Inductively Coupled Plasma Atomic Emission
54 Spectrometry (ICP-AES) at Peking University for samples collected in 2012 and 2013. Anions of
55 nitrate (NO_3), sulfate (SO_4) and chloride (Cl) were measured using ion chromatography (IC) at
56 Peking University. Major anions and cations concentrations were measured using IC at Southern
57 University of Science and Technology for samples collected in 2018.

58 **Text S2. Experimental Procedure of Soil Incubation.**

59 At the start of the second incubation in the reactor, 100 g of wet soil was weighed and added
60 to a glass reactor and filled with 5L CO_2 -free MQ water without headspace at room temperature.
61 The reactor was kept in dark for 80 hours, with a peristaltic pump running at 29 ml/min to ensure
62 mixing. The inlet and outlet of the reactor were connected with 6M NaOH solution to maintain
63 CO_2 -free headspace (Fig. S1). A total of 29 samples were collected at an interval of 30 min in the
64 initial 4.6 hours, at an interval of 60 min till 12 hours, and at an interval of 180 min until the end
65 of incubation that lasted 80 hours. At each sampling time, approximately 75 ml of water was
66 removed. Water volume and pH were measured immediately before filtering with 0.22 μm SPE
67 filters. Filtered samples were analyzed for DOC concentrations, UV-vis and fluorescence as in
68 section 2.2 of the main text.

69 **Text S3. Soil Incubation Results.**

70 During the 80-hours dark incubation of the frost soil in the reactor, the carbon mass of DOC
71 decreases from 30 mg to 12 mg in the initial 12 hours (Fig. S6a). The utilization of aromatic DOC
72 is supported by the doubling of SUVA_{254} values concurrent with a 60% decrease in DOC mass in
73 the system between 0 to 12 hours (Fig. S6). From 12 hours to 80 hours, SUVA_{254} values instead
74 decreased with an increase of DOC mass from 12 mg to 18 mg (Fig. S6c). The EEMs of all incubation
75 samples show the main fluorescent peak at excitation of 230 nm and emission of 240 nm,
76 suggesting that protein-like fluorophores are significant.

77

78

79

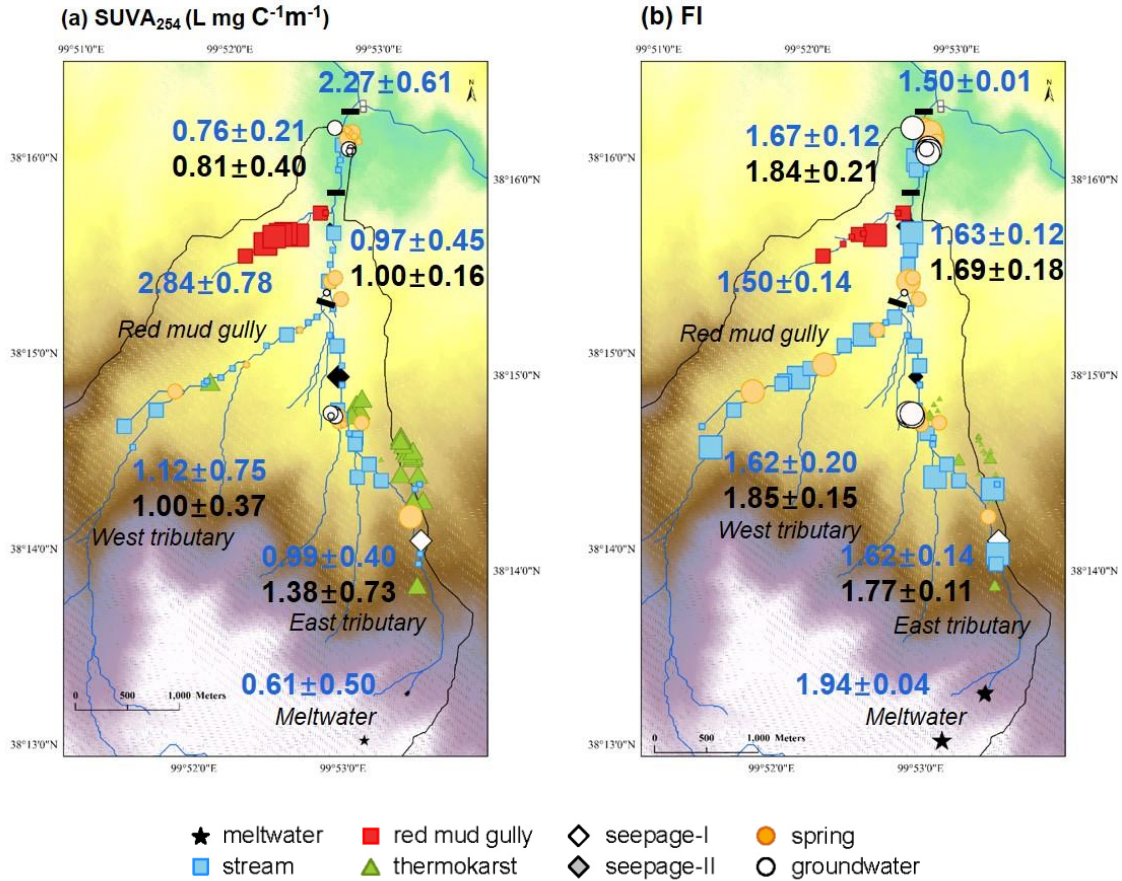
80

81

82

83

The first-order kinetic equation was applied to fit the SOC degradation curves for the decrease in DOC mass in the first 12 hrs (Fig. S6c). The half-time of soil derived DOC degradation is estimated to be 5 hours, and the degradation constant is calculated as dividing $-\ln(0.5)$ by half-time. Therefore, the degradation constant following first-order kinetics of DOC derived from permafrost soil is estimated to be 0.32 d^{-1} at 20°C , and is corrected to 0.11 d^{-1} for 5°C .



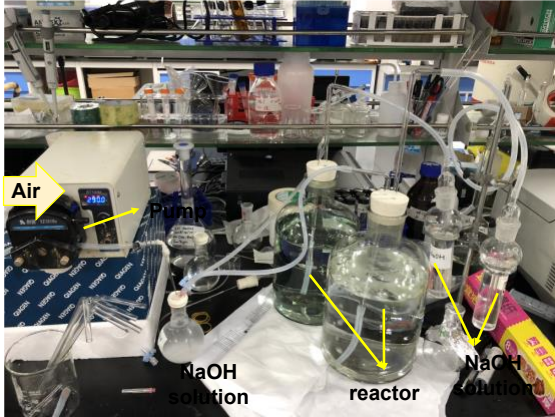
84

85 **Figure S1.** (a) SUVA₂₅₄ for eight types of water in HLGW, Qinghai-Tibetan Plateau. Small, medium
 86 and large symbol sizes indicate low (< 0.91 L mg C⁻¹ m⁻¹), medium (0.91–2.46 L mg C⁻¹ m⁻¹) and
 87 high (>2.46 L mg C⁻¹ m⁻¹) SUVA₂₅₄ according to tertile values of the entire dataset. Numbers are
 88 mean value ± one standard deviation for SUVA₂₅₄ in stream (blue) and subsurface water (black).
 89 (b) FI with small, medium and large symbol sizes indicate low (<1.59), medium (1.59–1.69) and
 90 high (>1.69) according to tertile values. Numbers are mean value ± one standard deviation for FI
 91 in stream (blue) and subsurface water (black).

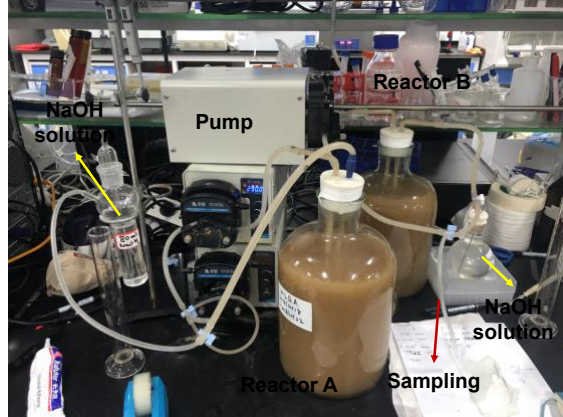
92

93

(a) Preparation of CO₂-free MQ water

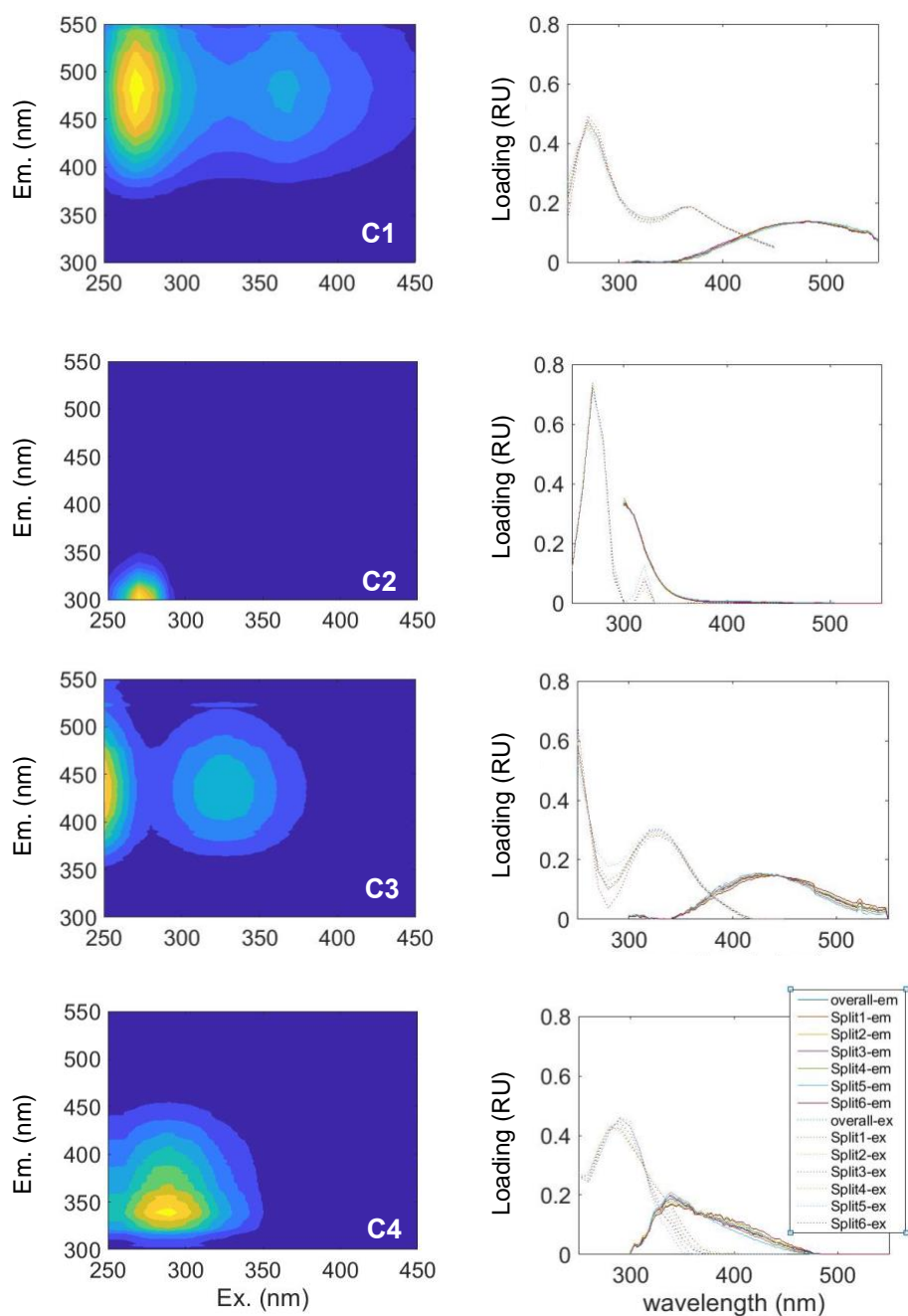


(b) Incubation reactor setting up and sampling



94

95 **Figure S2.** Figure S1. Experimental set up of frost soil reactor incubation. Left photo shows the
96 preparation of CO₂-free water for the two reactors. Right photo shows ongoing experiment with
97 sampling port location during incubation. The reactors used 5-L glass containers with inlet and
98 outlet ports. Continuous mixing is ensured by pumping water at a rate of 29 mL min⁻¹ from the
99 reactors by a peristaltic pump through a CO₂-free chamber. Samples were collected by a syringe
100 at the sampling port with a three-way valve.

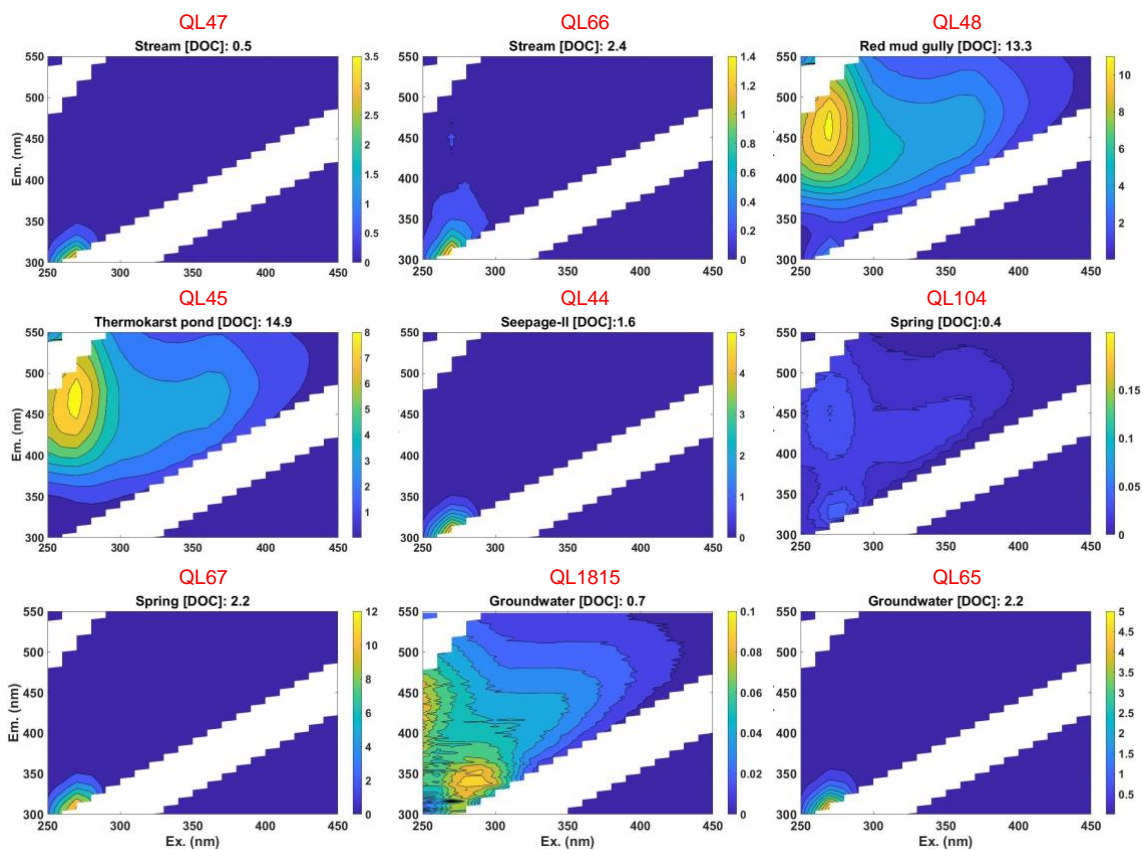


101

102 **Figure S3.** Fluorescence matrixes of the four identified components (left) and loadings of
 103 excitation (the dot lines) and emission (the solid lines) wavelength (right), respectively.
 104 Component 1 (ex: 270/370 nm, em: 470 nm) and component 3 (ex: <250/330 nm, em:420 nm)
 105 represent two humic-like components. Fluorescence characteristic of C2 (ex: 270 nm, em: 304
 106 nm) represents tyrosine-like material [D'Andrilli et al., 2019] (20), and C4 (ex: 290 nm, em: 338
 107 nm) represents amino-acids, free or bound in proteins compounds [Catala et al., 2015; Murphy
 108 et al., 2008].

109

110

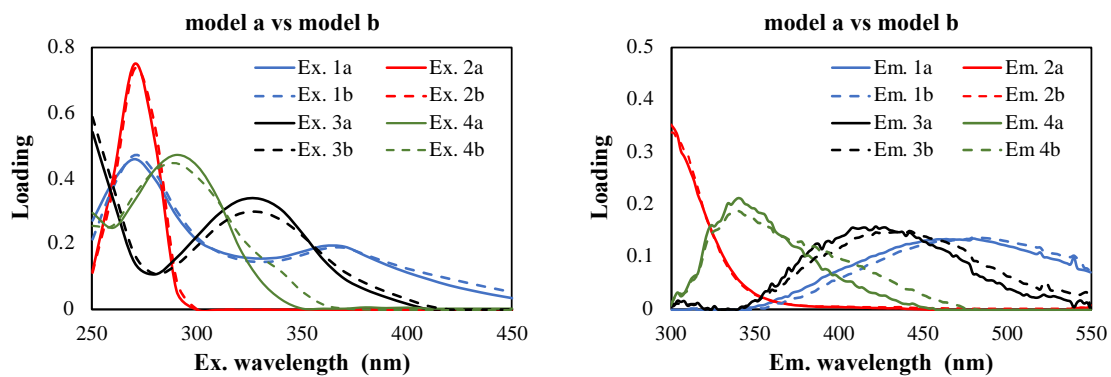


111

112 **Figure S4.** EEMs plots of typical stream, red mud gully, thermokarst pond, seepage-II, spring and
113 groundwater samples in HLGW. Sample ID is written in red (see Data set S1 for details), and the
114 DOC concentration (mg L^{-1}) is written in black above each EEMs. Color bar represents the
115 fluorescence intensity.

116

117

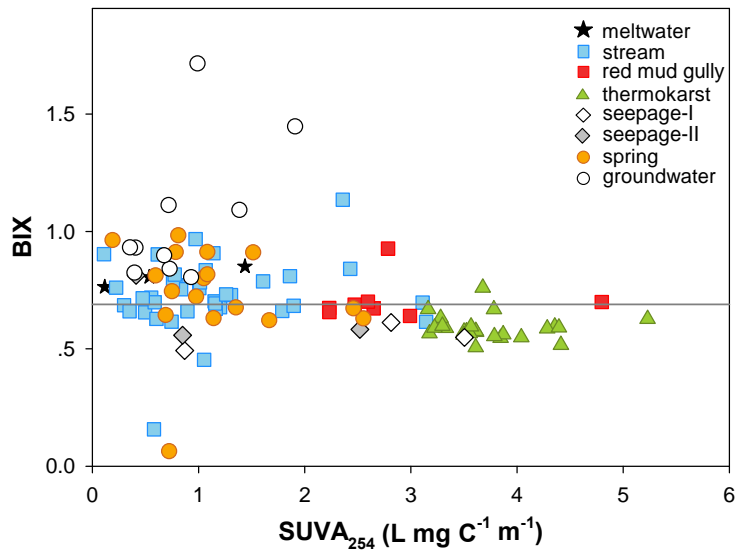


118

119 **Figure S5.** Comparison of excitation (Ex.) and emission (Em.) loadings of the four-components
120 models.

121

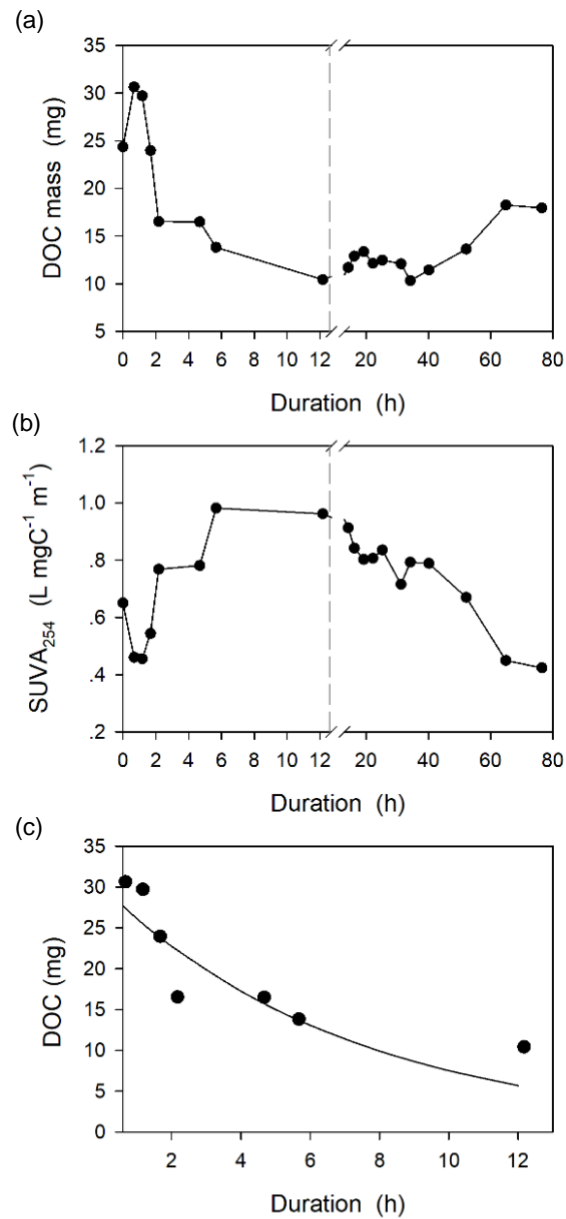
122



123

124 **Figure S6.** SUVA₂₅₄ vs BIX for eight types of water samples with gray line indicating the median
125 value of BIX for entire dataset.

126



128

129 **Figure S7.** Changes of (a) DOC expressed as carbon mass in supernatant and (b) SUVA₂₅₄ values
 130 over 80 hrs for the reactor soil incubation experiment in dark. The first-order kinetics fit to the
 131 soil carbon derived DOC degradation data in the first 12 hrs is shown in (c).
 132

Sample ID	Type	f_G	f_P	f_S	W_G	W_P	W_S	Sample ID	Type	f_G	f_P	f_S	W_G	W_P	W_S
QL41	stream	0.20	0.73	0.08	0.48	0.46	0.02	QL67	spring	0.23	0.61	0.17	0.37	0.36	0.03
QL42	stream	0.26	0.68	0.06	0.35	0.34	0.02	QL71	spring	0.23	0.71	0.06	0.36	0.35	0.03
QL43	stream	0.31	0.65	0.04	0.49	0.47	0.02	QL72	spring	0.29	0.66	0.05	0.39	0.38	0.02
QL47	stream	0.26	0.68	0.06	0.42	0.41	0.02	QL88	spring	0.27	0.56	0.17	0.42	0.41	0.03
QL58	stream	0.22	0.73	0.05	0.38	0.36	0.02	QL104	spring	0.30	0.53	0.18	0.45	0.44	0.03
QL61	stream	0.24	0.73	0.04	0.40	0.38	0.02	QL1812	spring	0.22	0.61	0.17	0.36	0.35	0.03
QL64	stream	0.23	0.72	0.05	0.39	0.37	0.02	QL1813	spring	0.18	0.66	0.16	0.32	0.31	0.03
QL66	stream	0.24	0.66	0.10	0.39	0.38	0.02	QL1818	spring	0.23	0.58	0.19	0.37	0.36	0.03
QL68	stream	0.21	0.72	0.07	0.37	0.35	0.02	QL1819	spring	0.22	0.59	0.19	0.36	0.35	0.03
QL73	stream	0.23	0.59	0.18	0.37	0.36	0.03	QL1820	spring	0.21	0.61	0.18	0.35	0.34	0.03
QL83	stream	0.27	0.59	0.13	0.43	0.42	0.02	QL1821	spring	0.22	0.61	0.16	0.37	0.36	0.03
QL84	stream	0.25	0.64	0.11	0.40	0.39	0.02	QL1830	spring	0.31	0.64	0.05	0.48	0.46	0.02
QL85	stream	0.27	0.60	0.13	0.42	0.41	0.02	QL1831	spring	0.22	0.61	0.17	0.46	0.45	0.02
QL86	stream	0.26	0.61	0.13	0.42	0.40	0.02	QL65	groundwater	0.21	0.62	0.17	0.35	0.34	0.03
QL87	stream	0.22	0.62	0.16	0.36	0.35	0.02	QL94	groundwater	0.27	0.59	0.14	0.42	0.41	0.03
QL90	stream	0.30	0.54	0.16	0.47	0.45	0.03	QL95	groundwater	0.27	0.58	0.14	0.43	0.42	0.03
QL92	stream	0.29	0.55	0.16	0.44	0.43	0.03	QL98	groundwater	0.11	0.74	0.15	0.27	0.26	0.02
QL99	stream	0.26	0.66	0.08	0.42	0.40	0.02	QL1808	groundwater	0.17	0.66	0.17	0.31	0.31	0.03
QL100	stream	0.26	0.65	0.09	0.42	0.40	0.02	QL1809	groundwater	0.17	0.67	0.17	0.31	0.30	0.03
QL101	stream	0.25	0.66	0.09	0.41	0.40	0.02	QL1810	groundwater	0.21	0.59	0.20	0.34	0.33	0.03
QL102	stream	0.25	0.66	0.09	0.40	0.39	0.02	QL1811	groundwater	0.17	0.69	0.14	0.32	0.31	0.02
QL103	stream	0.25	0.66	0.09	0.40	0.39	0.02	QL1815	groundwater	0.20	0.60	0.20	0.34	0.33	0.03
QL106	stream	0.22	0.67	0.12	0.36	0.35	0.02	QL1840	groundwater	0.22	0.63	0.15	0.37	0.35	0.03
QL1814	stream	0.29	0.57	0.14	0.44	0.43	0.03	QL1841	groundwater	0.22	0.63	0.15	0.36	0.35	0.03
QL1816	stream	0.27	0.59	0.14	0.43	0.42	0.03	QL1842	groundwater	0.21	0.64	0.15	0.35	0.34	0.03
QL1817	stream	0.26	0.59	0.15	0.42	0.40	0.03								
QL1829	stream	0.29	0.66	0.05	0.46	0.44	0.02								
QL1832	stream	0.32	0.61	0.08	0.49	0.47	0.02								
QL1833	stream	0.31	0.61	0.08	0.48	0.46	0.02								
QL1834	stream	0.25	0.60	0.15	0.40	0.39	0.03								
QL1836	stream	0.45	0.50	0.04	0.68	0.66	0.03								
QL1837	stream	0.38	0.50	0.12	0.58	0.56	0.03								
QL1838	stream	0.23	0.68	0.09	0.38	0.37	0.02								
QL1839	stream	0.35	0.50	0.15	0.54	0.52	0.03								
QL1844	stream	0.50	0.46	0.04	0.75	0.72	0.03								

134

135 **Table S1.** Unmixed fractions of glacier-snow (f_G), precipitation (f_P) and soil (f_S) endmember
136 contributions and the associated uncertainties for glacier-snow (W_G), precipitation (W_P) and soil
137 (W_S). For isotopic and EC “conservative” tracer concentrations and other chemical data of each
138 sample, see Dataset S1 and S2.

139

Depth b.s.l	Time (d)	DOC (mg/L solution)	DOC (mg/g wet soil)	SUVA ₂₅₄ (L mg C ⁻¹ m ⁻¹)	Protein- like percent	FI	BIX	Protein- like intensity (RU)
profile 1: thawed soil in seasonal permafrost zone near red mud gully (38.2630N, 99.8777E, 2850 m a.s.l)								
5 cm	3	13.1	0.05	3.48		1.33	0.48	
	40	282.8	1.10	0.88		1.41	0.47	
15 cm	3	10.0	0.04	3.53	22%	1.29	0.52	0.12
	40	125.4	0.35	0.98	11%	1.53	0.52	0.10
30 cm	3	13.6	0.02	3.79	29%	1.38	0.60	0.25
	40	16.1		3.87	13%	1.50	0.52	0.12
50 cm	3	27.8	0.05	1.71	42%	1.54	0.69	0.45
	40	33.1	0.06	1.88	13%	1.50	0.52	0.12
profile 2: dried thermokarst sediment (38.2423N, 99.8859 E, 3500 m a.s.l)								
10 cm	3	15.4	0.24	4.07	22%	1.33	0.53	0.22
	40	34.4	0.13	6.13	7%	1.41	0.48	0.17
30 cm	3	15.6	0.03	2.92	33%	1.51	0.60	0.34
	40	23.6	0.05	4.27	19%	1.43	0.54	0.13
80 cm	3	16.6	0.03	2.83	33%	1.47	0.58	0.39
	40	34.0	0.05	2.98	22%	1.35	0.53	0.18
profile 3: wet thermokarst sediment (38.2443N, 99.8879 E, 3500 m a.s.l)								
10 cm	1	18.7	0.06	1.48	20%	1.43	0.48	0.13
	3	44.8	0.14	1.33	10%	1.38	0.46	0.05
	40	46.8	0.16	4.18	6%	1.42	0.49	0.07
20 cm	1	28.0	0.07	2.08	19%	1.43	0.50	0.17
	3	53.3	0.14	1.93	9%	1.31	0.44	0.06
	40	42.5	0.12	4.40	9%	1.34	0.50	0.10
30 cm	1	23.1	0.06	2.51	19%	1.45	0.49	0.20
	3	63.5	0.16	1.80	9%	1.41	0.50	0.09
	40	38.9	0.11	4.44	7%	1.36	0.47	0.10
profile 4: permafrost zone (38.2414N, 99.8862E, elevation: 3600 m)								
5 cm	1	12.4	0.09	3.64	18%	1.29	0.42	0.11
	3	24.4	0.20	2.91	61%	1.35	0.48	1.17
	40	129.5	0.80	1.29	40%	1.45	0.55	0.58
15 cm	1	13.4	0.06	3.80	17%	1.30	0.42	0.11
	3	15.3	0.06	4.45	15%	1.29	0.48	0.14
	40	55.4	0.27	2.42	13%	1.40	0.50	0.11
25 cm	1	15.8	0.08	2.92	21%	1.27	0.43	0.13
	3	18.0	0.09	3.20	13%	1.30	0.45	0.11
	40	99.2	0.57	1.64	20%	1.38	0.55	0.21
35 cm	1	11.6	0.05	5.05	20%	1.32	0.43	0.15
	3	18.9	0.07	4.30	19%	1.27	0.48	0.20
	40	32.5	0.11	3.38	23%	1.38	0.56	0.15

140

141 **Table S2.** DOC concentrations and fluorescence properties for four soil profiles in soil batch
142 incubation experiment after 1, 3 and 40 extraction days.

143

144 **Dataset S1.** Detailed sampling information including water types, sampling date
145 (year/month/date), locations (Lat., Long, and Elev.), electrical conductivity (EC, $\mu\text{S}/\text{cm}$).
146 Calculations including proportions of glacier-snow meltwater, precipitation, and frozen soil
147 meltwater end members (G, P, S) based on stable isotopes and EC, the expected initial DOC (DOC_0)
148 and utilized DOC (ΔDOC). DOC concentrations (mg L^{-1}) and DOM optical parameters including
149 SUVA_{254} ($\text{L mg C}^{-1}\text{m}^{-1}$), fluorescence index (FI), freshness index (BIX), percentage proportions of
150 protein-like component (%) derived from PARAFAC.

151

152 * Only DOC concentrations were available for samples collected in Apr 2012. One thermokarst
153 sample collected near the west tributary was excluded in the data analysis.

154 ‡ The 7 groundwater samples were collected from the same monitoring well screened at 30 m at
155 the outlet (see MW in Fig.1d and Fig 3).

156 † The four groundwater samples were collected from the WW3 well (see WW3 in Fig.1d) located
157 in piedmont sloping plain dominated by seasonal frost, with screened intervals being 5, 10, 20
158 and 30 m underground, respectively.

159 § The groundwater/well water was collected from the WW4 with depth at 1m without pumping.

160 † The groundwater sample was collected from the WW1 well screened at 25 m (WW1 in Fig.1d).

161

162

163 **Dataset S2.** Additional field measurements including water temperature, pH, alkalinity (Alk, meq
164 L^{-1}), dissolved oxygen (DO, mg L^{-1}). Concentrations of major ions and total nitrogen (TN, mg L^{-1}).
165 The intensity loadings of the four components derived from PARAFAC (C1 to C4).

166

167 **Reference**

168

169 Catala, T. S., et al. (2015), Turnover time of fluorescent dissolved organic matter in the
170 dark global ocean, *Nature Communications*, 6.

171 D'Andrilli, J., J. R. Junker, H. J. Smith, E. A. Scholl, and C. M. Foreman (2019), DOM
172 composition alters ecosystem function during microbial processing of isolated sources,
173 *Biogeochemistry*, 142(2), 281-298.

174 Gran, G. (1952), Determination of the equivalence point in potentiometric titrations. Part
175 II, *Analyst*, 77(920), 661-671.

176 Murphy, K. R., C. A. Stedmon, D. T. Waite, and G. M. Ruiz (2008), Distinguishing
177 between terrestrial and autochthonous organic matter sources in marine environments
178 using fluorescence spectroscopy, *Marine Chemistry*, 108(1-2), 40-58.

179